Multiscale Properties of Instantaneous Parasympathetic Activity in Severe Congestive Heart Failure: a Survivor vs Non-Survivor Study

G. Valenza*,#, H. Wendt*, K. Kiyono, J. Hayano, E. Watanabe, Y. Yamamoto, P. Abry**, R. Barbieri**

Abstract— **Multifractal analysis of cardiovascular variability series is an effective tool for the characterization of pathological states associated with congestive heart failure (CHF). Consequently, variations of heartbeat scaling properties have been associated with the dynamical balancing of nonlinear sympathetic/vagal activity. Nevertheless, whether vagal dynamics has multifractal properties yet alone is currently unknown. In this study, we answer this question by conducting multifractal analysis through wavelet leader-based multiscale representations of instantaneous series of vagal activity as estimated from inhomogeneous point process models. Experimental tests were performed on data gathered from 57 CHF patients, aiming to investigate the automatic recognition accuracy in predicting survivor and non-survivor patients after a 4 years follow up. Results clearly indicate that, on both CHF groups, the instantaneous vagal activity displays power-law scaling for a large range of scales, from $\simeq 0.5$s to $\simeq 100$s. Using standard SVM algorithms, this information also allows for a prediction of mortality at a single-subject level with an accuracy of 72.72%.**

I. Introduction

Fractal theory has been giving a major contribution in understanding complex biological dynamics, especially involving nonlinear cardiovascular control and related autonomic nervous system (ANS) activity [1]–[7]. In fact, the cardiovascular system exhibits fractal complexity at many spatial and temporal scales. At the cellular level, for instance, fractal structure and functional behaviour are associated with the cardiac myocyte, whereas at a genome level fractal analysis has been providing meaningful information in case of inherited heart muscle disease hypertrophic cardiomyopathy and the so-called junk-DNA [1].

At a macroscopic level, fractal processes and multifractal models were successfully employed to model the temporal fluctuations in heartbeat dynamics [2], [4], [6], [7], whose direct clinical application has been directed to congestive heart failure (CHF) [4], [6], [8]–[10]. Particularly, it has been demonstrated that features of heartbeat dynamics derived from the time and frequency domain transformations are not sufficient to properly characterize the status of CHF patients, as there is the need of complementary nonlinear/multiscale metrics (cf., [4], [6], [9], [10] and references therein for reviews).

As the mentioned previous studies focused on multifractal analysis of heartbeat dynamics (through the analysis of heart rate variability series, HRV) exclusively, there still are questions left unanswered. In fact, it is unknown whether such scaling properties arise from the nonlinear/complex interactions between sympathetic and parasympathetic activity at the level of the sinoatrial node (as thoroughly reported in [11]), or whether there are already intrinsic multifractal properties in each autonomic dynamics *per se*. To this end, we here study multiscale properties of vagal activity as estimated with high resolution in time.

We use a powerful and robust methodology for conducting multifractal analysis, which employs multiscale representation and the so-called wavelet p-leaders, i.e., local ℓ^p norms of fractionally integrated wavelet coefficients [5], [12]. These multiscale quantities are known to better capture fluctuations of regularity in heartbeat data by scanning all details finer than the chosen analysis scale [2], [7].

Recently, we studied the impact of several interpolation strategies on wavelet leader based multiscale representations applied to heartbeat interval series [13]. We demonstrated that such representations may be biased by the kind of interpolation employed (e.g., linear, spline, etc.), therefore an ad-hoc physiologically plausible modelling is strongly recommended. We proposed the use of inhomogeneous point-processes to effectively characterize the probabilistic generative mechanism of heartbeat events, even considering short recordings under nonstationary conditions [14]. The unevenly spaced heartbeat intervals are then represented as observations of a state-space point process model defined at each moment in time, thus allowing to estimate instantaneous HRV measures, including instantaneous vagal activity, without using any disruptive interpolation method.

Experimental tests are performed on data comprising 57 CHF patients, aiming to accurately assess the risk of posterior mortality by automatically discerning and predicting patients surviving more than 4 years after heart failure.

II. Materials and Methods

A. Point-Process Models of Heartbeat Dynamics

A random point process is a stochastic process comprising the occurrence of discrete events in time. In particular, this model defines the probability density functions (PDFs) predicting a future event, given a parametric formulation of the current and past observations. Here, point-process

Work supported by ANR-16-CE33-0020 MultiFracs and CNRS PICS #7260 MATCHA, France.

G. Valenza is with the Bioengineering and Robotics Research Center E. Piaggio and also with the Department of Information Engineering, University of Pisa, Pisa, Italy (g.valenza@ieee.org); H. Wendt is with IRIT-ENSEEIHT, Université de Toulouse, CNRS, France, herwig.wendt@irit.fr; P. Abry is with Physics Dept., ENS Lyon, CNRS, France, patrice.abry@ens-lyon.fr; K. Kiyono is with the Osaka University, Japan, kiyono@bpe.es.osaka-u.ac.jp; J. Hayano is with the Department of Medical Education, Nagoya City University Graduate, School of Medical Sciences, Japan, hayano@med.nagoya-cu.ac.jp; E. Watanabe is with the Department of Cardiology, Fujita Health University School of Medicine, Toyoake, Japan, enwatan@fujita-hu.ac.jp, Y. Yamamoto is with the University of Tokyo, Japan, yamamoto@p.u-tokyo.ac.jp; R. Barbieri is with the Department of Electronics, Informatics and Bioengineering, Politecnico di Milano, Milano, Italy, riccardo.barbieri@polimi.it

* First Authors. # Corresponding author. ** Senior authors.

stochastic events are represented by heartbeats (i.e., the time occurrence of R-waves in ECGs), therefore aiming to characterize the PDF of the next ventricular contraction given a linear combination of the past RR intervals. Motivated by physiological and modelling reasons, such PDFs are known to be inverse-Gaussian (IG) distributions [14].

Therefore, we model the unevenly sampled RR interval series through IG PDFs whose first order moment (the mean $\mu_{\mathrm{RR}}(t, \mathcal{H}_t, \xi(t))$, with $\mathcal{H}_t$ as the history of past RR intervals, $\xi(t)$ the vector of the time-varying parameters, and $\xi_0(t)$ the shape parameters of the IG) has a linear autoregressive formulation. As a major advantage, since such PDFs are mathematically defined in continuous time, we can obtain instantaneous measures without applying any interpolation techniques to the original RR interval series. Importantly, this advantage applies also for the derivation of spectral measures, following the estimation of $\mu_{\mathrm{RR}}(t, \mathcal{H}_t, \xi(t))$ and kernels therein.

Formally:

$$\mu_{\mathrm{RR}}(t, \mathcal{H}_t, \xi(t)) \;=\; \gamma_0 \;+\; \sum_{i=1}^{p} \gamma_1(i,t)\, \mathrm{RR}_{\widetilde{N}(t)-i} \qquad (1)$$

where $\widetilde{N}(t)$ is the left continuous sample path of the associated counting process (i.e., the index of the previous R-wave event before time t), $\mathcal{H}_t = (u_j, \mathrm{RR}_j, \mathrm{RR}_{j-1}, ..., \mathrm{RR}_{j-p+1})$, $\xi(t) = [\xi_0(t), \gamma_0(t), \gamma_1(1,t), ..., \gamma_1(p,t)]$, and $\xi_0(t) > 0$.

We effectively estimate the parameter vectors $\xi^a(t)$ at each time interval $\Delta = 5ms$ using the Newton-Raphson procedure to compute the local maximum-likelihood estimate [14]. Because there is significant overlap between adjacent local likelihood intervals, we start the Newton-Raphson procedure at t with the previous local maximum-likelihood estimate at time $t - \Delta$.

We determine the optimal model order $\{p\}$ by prefitting the point process model goodness-of-fit to a subset of the data [14]. Model goodness-of-fit is based on the Kolmogorov-Smirnov (KS) test and associated KS statistics [14]. The recursive, causal nature of the estimation allows to predict each new observation, given the previous history, independently at each iteration. The model and all its parameters are therefore also updated at each iteration, without priors. In other words, each test point RR_k is tested against one instance of a time-varying model trained with points $\{\mathrm{RR}_j\}$ with $j < k$. Autocorrelation plots are also considered to test the independence of the model-transformed intervals [14]. Once the order $\{p\}$ is determined, the initial model coefficients are estimated by the method of least squares [14]. Extensive details on this modelling can be found in [14]

B. Multiscale analysis

1) Self-similarity and wavelets: Classical multiscale analysis relies on the estimation of wavelet coefficients, which are obtained by comparing a series of RR intervals $\{RR\}$ to the collection $\{\psi_{j,k}(t) = 2^{-j}\psi(2^{-j}t - k)\}_{(j,k)\in\mathbb{N}^2}$ of dilated and translated templates of a mother wavelet ψ via inner products, $d_{\{RR\}}(j,k) = \langle \psi_{j,k} | \{RR\} \rangle$ (see, e.g., [15] for details on wavelet transforms).

For *self-similar* processes such as fractional Brownian motion, which are commonly used models for HRV series [8], the so-called wavelet *structure functions* $S(j,q)$ display power laws with respect to scale j

$$S(j,q) = \sum_{k=1}^{n_j} |d_{\{RR\}}(j,k)|^q \simeq K_q 2^{jqH} \qquad (2)$$

with n_j the number of $d_{\{RR\}}(j,k)$ available at scale 2^j. The Hurst parameter H and the function $S(q=2,j)$ are directly related to the distribution of energy along frequencies (i.e., to the Fourier spectrum or autocorrelation of $\{RR\}$). They are hence linear features of $\{RR\}$ that can be efficiently estimated using wavelets [2], [5].

2) Multifractal models and wavelet p-leaders: It has been demonstrated that self-similar models describe only parts of the scaling properties in HRV data and that *multifractal* models could provide more complete descriptions (see, e.g., [2], [4]). These essentially imply that the linear scaling exponents qH in (4) should be replaced with a more flexible, concave function $\zeta(q)$, and that the parameter H alone can no longer account for all scaling properties in HRV data. To correctly estimate $\zeta(q)$, wavelet coefficients must be replaced with non-linear multiscale quantities that sense the local regularity fluctuations in data across all finer scales [5]. In this study, we employ the wavelet *p-leaders*, which have recently renewed the state-of-the-art for the estimation of multifractal models [12]. They are defined as ℓ^p-norms of (fractionally integrated of order γ) wavelet coefficients in a narrow time neighborhood over all finer scales

$$L^{(p,\gamma)}_{\{RR\}}(j,k) = \left(2^j \sum\nolimits_{\lambda' \subset 3\lambda_{j,k}} |2^{j'\gamma} d_X(\lambda')|^p 2^{-j'}\right)^{1/p}, \quad (3)$$

with $\lambda_{j,k} = [k2^j, (k+1)2^j)$ and $3\lambda_{j,k} = \bigcup_{m\in\{-1,0,1\}} \lambda_{j,k+m}$. The parameters $\gamma \geq 0$ and $p > 0$ must be chosen to ensure minimal regularity constraints (cf. [12] and references therein for details on multifractal analysis, beyond the scope of this contribution). It can been shown that the multifractal properties of $\{RR\}$ are well described by a multiscale representation consisting of the sample cumulants Cum_m of the logarithm of p-leaders $\ln L^{(p,\gamma)}(j,\cdot)$ [5]

$$C_m^{(p,\gamma)}(j) \equiv \; \mathrm{Cum}_m \ln L^{(p,\gamma)}(j) \simeq c_m^0 + c_m \ln 2^j. \qquad (4)$$

In particular, the coefficients c_m are related to $\zeta(q)$ via the polynomial expansion $\zeta(q) \equiv \sum_{m\geq 1} c_m q^m/m!$ (and hence to the multifractal spectrum, cf., [5] for details). Consequently, the leading coefficients c_1 and $C_1^{(p,\gamma)}(j)$ are closely related to H and $S(2,j)$, respectively, and constitute linear features associated to the autocorrelation of $\{RR\}$ [2], [5], while $C_2^{(p,\gamma)}(j)$ and $C_3^{(p,\gamma)}(j)$ (the variance and skewness of $\ln L^{(p,\gamma)}(j)$, respectively) and c_2 and c_3 (related to the multifractal properties of $\{RR\}$) are nonlinear features that capture information beyond correlation.

C. Experimental Data

24-hour Holter ECG recordings from a cohort of 57 patients suffering from CHF were made available by the Fujita Health University Hospital, Japan. A total of 28 of these patients died within 33 ± 17 months (range, 1-59

months) after Hospital discharge, whereas 27 survived for a longer time (see [3] for further clinical details). Below, the former group will be referred to as non-survivors (NS) and the latter as survivors (SV). Two recordings were discarded due to poor signal quality. From the ECG recordings, R peak arrival times were automatically extracted for each patient, and missing data and outliers stemming from atrial or ventricular premature complexes were handled by automated preprocessing tools. None of the subjects considered in this study present sustained tachyarrhythmias.

D. Analysis setting, Statistical Testing, and Pattern Recognition

Instantaneous series of $\mu_{\mathrm{RR}}(t, \mathcal{H}_t, \xi(t))$ are estimated from the $\{RR\}$ interval series through the point-process method previously described. The instantaneous autospectrum $Q(t,f)$ is obtained directly from the instantaneous kernels $[\gamma_1(1,t), ..., \gamma_1(p,t)]$. Then, we can compute the instantaneous index within the low frequency (LF = 0.04-0.14 Hz) and high frequency (HF = 0.14-0.4 Hz) ranges [14]. Instantaneous series of HF power are taken as marker of vagal activity and, then, analyzed using the p-leaders based multiscale representations. The analysis is conducted using Daubechies3 wavelets. Further, p-leaders with $p = 1$, which have been shown to yield lowest variance [12], are used. Moreover, inspection of the database leads to the choice $\gamma = 1$. In what follows, we compactly write $C_m(j)$ for $C_m^{(p,\gamma)}(j)$ [1].

To average among groups, we condensed the information about the time-varying dynamics of a given instantaneous feature through its median value. We then evaluated between-group differences (NS vs. SV) for every feature using bivariate non parametric statistics (Mann-Whitney test) under the null hypothesis that the between-subject medians of the two groups are equal.

Furthermore, we employed an automatic classification algorithm based on well-known Support Vector Machine (SVM) in order to automatically discern NS vs. SV at a single subject level. We use the following feature sets:

- α set: a subset of multiscale representation $\log_2 S(2,j), C_1(j), C_2(j), C_3(j)$ for $j \in [j_m, j_M]$
- β set: a subset of exponents $\zeta(2), c_1, c_2, c_3$, estimated for each range of scales

A multidimensional point in a given feature set was considered an outlier if z-scores associated to its dimensions were greater than 3. To assess the out-of-sample predictive accuracy of the system, we adopted a Leave-One-Out (LOO) procedure based on a SVM-based classifier. Specifically, we employed a nu-SVM (nu=0.5) with a radial basis kernel function with $\gamma = n^{-1}$, where n is equal to the number of features. Within the LOO scheme, the training set was normalized by subtracting the median value and dividing by the MAD over each dimension. These values were then used to normalize the example belonging to the test set. During the LOO procedure, this normalization step was performed on each fold. Classification results are summarized as balanced recognition accuracy (i.e., average of sensitivity and specificity).

[1]Note that it can be shown that, for a large subclass of multifractal processes, $C_1(j) \equiv C_1^{(p,\gamma)}(j) - \gamma \ln 2^j$ while $C_m^{(p,\gamma)}(j)$ for $m \geq 2$ does not depend on γ and p.

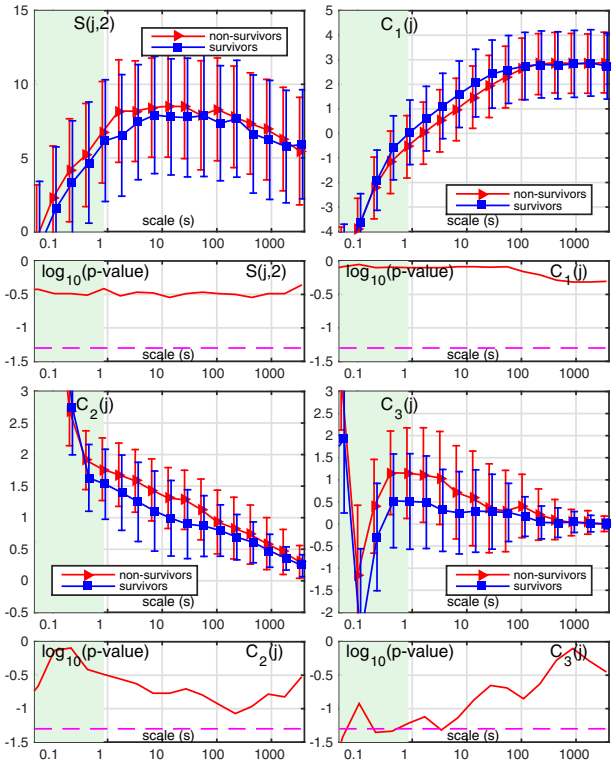

Fig. 1. Multiscale representations $S(j,2)$, $C_1(j)$, $C_2(j)$ and $C_3(j)$ for HF time series (median and mad) for survivors (blue squares) an non-survivors (red triangles) subjects (top panels); Wilcoxon rank-sum test p-values (bottom panels).

TABLE I

	NS: med	(mad)	SV: med	(mad)	p-value
$\zeta(2)$	-0.069	(0.223)	-0.013	(0.257)	0.36
c_1	0.566	(0.071)	0.528	(0.106)	0.40
c_2	-0.164	(0.122)	-0.165	(0.114)	0.62
c_3	-0.137	(0.243)	-0.075	(0.272)	0.63

Scaling and multifractal exponents $\zeta(2), c_1, c_2, c_3$ estimated over scales $[2.6, 81.9]s$ (median and mad; second and third columns) and Mann-Whitney p-values.

III. Experimental Results and Discussion

A. Scaling properties

In Fig. 1, the wavelet coefficient based $\log_2 S(2,j)$ and p-leader based log-cumulants $C_1(j), C_2(j), C_3(j)$ of the instantaneous HF power time series are plotted as a function of analysis scale $a = 2^j$. The shaded area indicates the time scales of finer resolution than the raw $\{RR\}$ interval data (below $j \leq 7$, i.e., smaller than $\simeq 0.8$s). The results clearly indicate that the instantaneous vagal activity displays power law scaling for a large range of scales, from $\simeq 0.5$s to $\simeq 100$s. These scaling properties are observed both for the NS and SV groups. Moreover, the associated exponents $\zeta(2)$ and c_m (estimated over scales $[2.6, 81.9]$s, summarized in Tab. I) show that the instantaneous HF power time series

can be well described by a multifractal model, since both c_2 and c_3 take on values that are different from zero.

Fig. 1 further indicates that the scaling laws of $C_1(j), C_2(j), C_3(j)$ of the NS and the SV group are slightly different for fine scales ($\simeq$ 0.5s to $\simeq$ 20s). To assess the independent and scale-wise discriminative power of the multiscale representation, p-values from Mann-Whitney test are computed and plotted in Fig. 1 (bottom panels; the dashed line indicates the value $p = 0.05$). None of the multiscale quantities $\log_2 S(2,j), C_1(j), C_2(j), C_3(j)$, considered individually, are significant for distinguishing NS from SV subjects. Similar conclusions are obtained for the scaling and multifractal exponent $\zeta(2), c_1, c_2, c_3$, which also yield large p-values (see Tab. I).

B. SV versus NS classification

We evaluated the LOO-SVM performance in predicting SV vs. NS patients using the feature sets α and β estimated from instantaneous HF series exclusively (constituting α_{HF} and β_{HF} sets), as well as from combined estimates of instantaneous μ_{RR} and HF power (constituting $\alpha_{[\mu_{RR},HF]}$ and $\beta_{[\mu_{RR},HF]}$ sets).

Classification performance (measured in terms of accuracies, i.e., % of overall — True Negative and True Positive — total correct classification) are reported in Table II. Considering the SV vs. NS classes, accuracy of 50% is the change.

TABLE II

CLASSIFICATION ACCURACY IN %

scale (j)	$\alpha_{[\mu_{RR},HF]}$ set	$\beta_{[\mu_{RR},HF]}$ set	α_{HF} set	β_{HF} set
5	69.09	40.00	43.64	43.64
6	65.45	50.91	60.00	**60.00**
7	56.36	**54.55**	52.72	50.91
8	56.36	40.00	**61.81**	56.36
9	54.54	41.82	61.81	36.36
10	**72.72**	43.64	61.81	36.36
11	63.63	50.91	47.27	29.09
12	65.45	45.45	47.27	50.90
13	61.81	38.18	45.45	41.82
14	52.72	-	43.64	-
15	49.09	-	40.00	-
16	52.73	-	38.18	-
17	49.09	-	47.27	-
18	49.09	-	29.09	-
19	61.82	-	40.00	-

Bold indicates best accuracy per feature set with $j_m = 5$, and $j_M = 19$.

Table II shows that multiscale representation of combined μ_{RR} and HF power ($\alpha_{[\mu_{RR},HF]}$ set) show the best recognition accuracy (up to 72.72%). Of note, best accuracy obtained from multiscale representation $\log_2 S(2,j), C_1(j), C_2(j), C_3(j)$ of instantaneous vagal activity is above the chance (up to 61.81%), although below the best accuracy obtained from the use of μ_{RR} alone (i.e., 65.45%; data not shown here, cf., [13]). Confusion matrix of the best recognition is shown in Table III.

TABLE III

SVM	SV	NS
SV	**78.57%**	21.43%
NS	33.34%	**66.66%**

Confusion matrix of SV vs. NS classification using $\alpha_{[\mu_{RR},HF]}$ set at scale $j = 10$

IV. CONCLUSION

In conclusion, we studied time series of instantaneous HF power (time resolution of 5ms) using multiscale analysis based on the recently introduced p-leader formalism. We demonstrated that, both on SV and NS patients, the instantaneous vagal activity displays power-law scaling for a large range of scales. This complements current knowledge which has been limiting multiscale dynamics to nonlinear sympathetic/parasympathetic interactions, thanks to the analysis of RR interval series. Using standard SVM algorithms, we leveraged on this information in order to achieve a prediction of mortality at a single-subject level with an accuracy of 72.72%. From a methodological view, these results strengthen the link between inhomogeneous point-process models of heartbeat dynamics and wavelet leader-based multiscale representation. In line with the current literature, this study poses a step forward for a diagnostic tool able to assess CHF morbidity and mortality. Future endeavours will focus on the study of a comprehensive set of point-process derived instantaneous linear and nonlinear features gathered from multiscale analyses, as well as on the investigation of optimal classification model and feature selection.

REFERENCES

[1] G. Captur, A. L. Karperien, A. D. Hughes, D. P. Francis, and J. C. Moon, "The fractal heart [mdash] embracing mathematics in the cardiology clinic," *Nature Reviews Cardiology*, 2016.

[2] M. Doret *et al.*, "Multifractal analysis of fetal heart rate variability in fetuses with and without severe acidosis during labor," *Am. J. Perinatol.*, vol. 28, no. 4, pp. 259–266, 2011.

[3] K. Kiyono *et al.*, "Non-gaussian heart rate as an independent predictor of mortality in patients with chronic heart failure," *Heart Rhythm*, vol. 5, no. 2, pp. 261–268, 2008.

[4] P. C. Ivanov *et al.*, "Multifractality in human heartbeat dynamics," *Nature*, vol. 399, no. 6735, pp. 461–465, 1999.

[5] H. Wendt *et al.*, "Bootstrap for empirical multifractal analysis," *IEEE Signal Proc. Mag.*, vol. 24, no. 4, pp. 38–48, 2007.

[6] Y. Yamamoto and R. L. Hughson, "On the fractal nature of heart rate variability in humans: effects of data length and beta-adrenergic blockade," *American Journal of Physiology-Regulatory, Integrative and Comparative Physiology*, vol. 266, no. 1, pp. R40–R49, 1994.

[7] H. Wendt *et al.*, "Multiscale wavelet p-leader based heart rate variability analysis for survival probability assessment in chf patients," in *Proc. Int. IEEE EMBS Conf.*, Chicago, USA, 2014, pp. 2809–2812.

[8] K. Kiyono, Z. R. Struzik, N. Aoyagi, S. Sakata, J. Hayano, and Y. Yamamoto, "Critical scale-invariance in healthy human heart rate," *Phys. Rev. Lett.*, vol. 93, p. 178103, 2004.

[9] U. R. Acharya, K. P. Joseph, N. Kannathal, C. M. Lim, and J. S. Suri, "Heart rate variability: a review," *Medical and Biological Engineering and Computing*, vol. 44, no. 12, pp. 1031–1051, 2006.

[10] G. Valenza, L. Citi, and R. Barbieri, "Estimation of instantaneous complex dynamics through lyapunov exponents: a study on heartbeat dynamics," *PloS one*, vol. 9, no. 8, p. e105622, 2014.

[11] K. Sunagawa, T. Kawada, and T. Nakahara, "Dynamic nonlinear vago-sympathetic interaction in regulating heart rate," *Heart and vessels*, vol. 13, no. 4, pp. 157–174, 1998.

[12] R. Leonarduzzi, H. Wendt, P. Abry, S. Jaffard, C. Melot, S. G. Roux, and M. E. Torres, "p-exponent and p-leaders, part ii: Multifractal analysis. relations to detrended fluctuation analysis." *Physica A*, vol. 448, pp. 319–339, 2016.

[13] G. Valenza *et al.*, "Point-process high-resolution representations of heartbeat dynamics for multiscale analysis: A chf survivor prediction study," in *Proc. of IEEE-EMBC*. IEEE, 2015, pp. 1951–1954.

[14] R. Barbieri, E. Matten, A. Alabi, and E. Brown, "A point-process model of human heartbeat intervals: new definitions of heart rate and heart rate variability," *American Journal of Physiology-Heart and Circulatory Physiology*, vol. 288, no. 1, p. H424, 2005.

[15] S. Mallat, *A wavelet tour of signal processing*. Academic press, 1999.